Human neural stem cells differentiate and promote locomotor recovery in spinal cord-injured mice

Brian J. Cummings*†, Nobuko Uchida‡§, Stanley J. Tamaki‡§, Desirée L. Salazar¶‖, Mitra Hooshmand¶‖, Robert Summers**, Fred H. Gage**, and Aileen J. Anderson*¶‖

Departments of *Physical Medicine and Rehabilitation and ¶Anatomy and Neurobiology and ‖Reeve-Irvine Research Center, University of California, Irvine, CA 92697; ‡StemCells, Inc., 3155 Porter Drive, Palo Alto, CA 94304; and **The Salk Institute for Biological Studies, 10010 North Torrey Pines Road, La Jolla, CA 92037

Communicated by Irving L. Weissman, Stanford University School of Medicine, Stanford, CA, August 16, 2005 (received for review December 15, 2004)

We report that prospectively isolated, human CNS stem cells grown as neurospheres (hCNS-SCns) survive, migrate, and express differentiation markers for neurons and oligodendrocytes after long-term engraftment in spinal cord-injured NOD-*scid* mice. hCNS-SCns engraftment was associated with locomotor recovery, an observation that was abolished by selective ablation of engrafted cells by diphtheria toxin. Remyelination by hCNS-SCns was found in both the spinal cord injury NOD-*scid* model and myelin-deficient *shiverer* mice. Moreover, electron microscopic evidence consistent with synapse formation between hCNS-SCns and mouse host neurons was observed. Glial fibrillary acidic protein-positive astrocytic differentiation was rare, and hCNS-SCns did not appear to contribute to the scar. These data suggest that hCNS-SCns may possess therapeutic potential for CNS injury and disease.

behavioral assessment | differentiation | stem cell transplantation

Recent studies have used a variety of immortalized, engineered, or isolated rodent-derived precursor/stem cells transplanted into rodent models of spinal cord injury. Many of these studies focused on cell survival and did not address differentiation, functional recovery, or the causal relationship between successful engraftment and observed behavioral improvements. When differentiation was investigated, embryonic and adult neural stem cells were reported to principally assume glial fibrillary acidic protein (GFAP)-positive astrocytic phenotypes after grafting into nonneurogenic regions of uninjured adult CNS (1, 2) or injured spinal cord (3–5). Furthermore, although *in vitro* predifferentiation paradigms designed to generate neural lineage restricted precursors successfully generated β-tubulin III (Tuj-1)-positive neuronal phenotypes either *in vitro* or after transplantation into uninjured spinal cord, this commitment was overridden by environmental cues in the injured spinal cord (6).

Transplants of human brain-derived stem cells or human spinal cord tissue into injured rat spinal cord have been described (7–9). Moreover, several human cell transplantation paradigms recently have been reported to promote locomotor recovery: human umbilical cell infusion in a rat spinal cord injury model, although only within 3 weeks or less postgrafting (10); neurons differentiated *in vitro* under retinoic acid from human embryonal teratocarcinoma cells and transplanted into a rat spinal cord injury model (11); human ES cells differentiated *in vitro* to oligoprogenitors and transplanted into a rat spinal cord injury model (12); and human neural stem/progenitor cells transplanted into a monkey spinal cord injury model (13). In general, these studies lack some or all of the following: definitive identification of transplanted cells, long-term survival and engraftment data, evidence of differentiation, and/or direct evidence of functional integration of human cells in the injured spinal cord. The current study addresses three previously unexplored issues in stem cell transplantation research for spinal cord repair in what are, to our knowledge, the first spinal cord injury experiments using prospectively isolated, human CNS stem cells grown as neurospheres (hCNS-SCns) derived from fetal brain (14, 15). First, we report that hCNS-SCns survive, engraft, differentiate, and are associated with locomotor improvements after traumatic spinal cord injury in NOD-*scid* mice. Second, we report that selective ablation of engrafted hCNS-SCns by diphtheria toxin (DT) results in loss of locomotor recovery. Third, we show that transplanted hCNS-SCns myelinate dysmyelinated axons in *shiverer* mutants, remyelinate axons in traumatically injured NOD-*scid* spinal cord, and differentiate into neurons exhibiting electron microscopic criteria consistent with synapse formation with mouse host neurons.

Methods

Further experimental details are given in *Supporting Text*, which is published as supporting information on the PNAS web site.

Contusion Injuries. Behavioral and histological data (collected in the same animals) from two cohorts are included in the results. Female NOD-*scid* mice received a laminectomy at vertebral level T9. One cohort received a 50-kilodyne (kd) (1 dyne = 10 μN) (n = 38) contusion spinal cord injury, and the second cohort received a 60-kd (n = 30) contusion spinal cord injury using an Infinite Horizon Impactor (Precision Systems and Instrumentation, Lexington, KY). Seven days after spinal cord injury, mice in the 50-kd cohort were tested by using the Basso, Beattie, and Bresnahan (BBB) rating scale and randomized to receive hCNS-SCns (n = 16) or vehicle (n = 19). Five hCNS-SCns-transplanted animals and 4 vehicle-injected animals were excluded by using prehoc criteria, resulting in 11 hCNS-SCns-grafted animals and 15 vehicle control animals. In the 60-kd cohort, mice were randomized to receive hCNS-SCns, human fibroblasts (hfibroblasts), or vehicle as above. Before analysis, 2 hCNS-SCns-transplanted animals and 2 hfibroblast-injected animals were excluded by using prehoc criteria, resulting in 8 hCNS-SCns, 8 hfibroblast, and 10 vehicle controls.

Human Cell Culture, Maintenance, and Injections. Long-term hCNS-SCns cultures from fetal brain are described in ref. 15. Neurospheres were concentrated to a density of 75,000 cells per μl in injection buffer consisting of 50% Hanks' balanced salt solution and 50% X-vivo medium. For cohort 2, hfibroblasts from fetal liver were grown to confluence in Iscove's modified Dulbecco's medium/10% FBS, dissociated with trypsin, washed, and concentrated to 75,000 cells per μl. Nine days after spinal cord injury, mice received four injections bilaterally 0.75 mm from midline at both the anterior aspect of T10 and the posterior aspect of T8. Each site received 250 nl of cells or vehicle. Functional recovery was assessed by using a modified (18 point) BBB locomotor rating scale weekly for 1 month and then biweekly (16, 17) by observers blind to

Freely available online through the PNAS open access option.

Abbreviations: SCI, spinal cord-injured; DT, diphtheria toxin; hCNS-SCns, human CNS stem cells grown as neurospheres; GFAP, glial fibrillary acidic protein; MBP, myelin basic protein; kd, kilodyne; BBB, Basso, Beattie, and Bresnahan; hfibroblast, human fibroblast.

†To whom correspondence should be addressed. E-mail: cummings@uci.edu.

§N.U. and S.J.T. are employees of StemCells, Inc., which stands to profit from this research.

treatment. At 16 weeks, a subset of animals was also videotaped on a horizontal ladder beam task in a series of three trials and scored blind for step errors. After BBB assessment at 16 weeks, mice received two i.p. injections of DT (50 μg/kg) 24 h apart, were reassessed on the BBB 1 week later, and were then euthanized according to the Institutional Animal Care and Use Committee guidelines at University of California, Irvine.

Perfusion and Tissue Collection. Mice were anesthetized and transcardially perfused with 30 ml of PBS followed by 100 ml of 4% paraformaldehyde. Spinal cords were dissected, and the segments corresponding to T2–T5, T6–T12, and T13–L3 were blocked. Blocks were postfixed overnight in 4% paraformaldehyde. For immunocytochemistry, some blocks were equilibrated in 30% sucrose/PBS for 12 h, embedded in OCT compound, and frozen at −65°C in isopentane for sectioning. For EM, 1-mm-thick coronal sections were postfixed in 4% glutaraldehyde immediately after paraformaldehyde fixation.

Immunocytochemistry. Immunostaining was conducted as described in ref. 18. SC101, a monoclonal antibody for human nuclei; SC121, a monoclonal antibody for human cytoplasm; and SC123, a monoclonal antibody specific for human GFAP, were produced by StemCells, Inc. Other primary antibodies included: β-tubulin III (Covance, Berkeley, CA); glutamate decarboxylase (GAD)-67, NeuN, NG2, and Neurofilament-150 (Chemicon); pan-GFAP (DAKO); Vimentin (Cell Marque, Hot Springs, AR); CC-1/APC (Oncogene); and myelin basic protein (MBP) 1-188 (Biogenesis, Bournemouth, U.K.). Secondary antibodies in double-labeling experiments were Alexa Fluor 488 and 555 from Molecular Probes. Confocal imaging was conducted by using a Bio-Rad Radiance 2000 system using LASERSHARP 2000 software with lambda strobing to reduce bleed-through associated with simultaneous scanning.

EM. Tissue was either cut at 50 μm on a Vibratome and immunostained with SC121 and diaminobenzidine or washed in 0.1 M sodium cacodylate buffer overnight, fixed with osmic acid, and embedded in Spurr resin.

NOD-*scid*/*shi* Crosses. The MBP^{shi} mutation was backcrossed for four generations onto the NOD-*scid* background. NOD-*scid*/*shi* mice received either intracerebellar grafting of hCNS-SCns at postnatal day 1–2 or a contusion injury to T9 at 6 weeks of age combined with hCNS-SCns or vehicle; survival was for 4 weeks.

Results

hCNS-SCns Survive and Engraft Within the Injured Spinal Cord of NOD-*scid* Mice. Mice receiving hCNS-SCns grafts were euthanized at 24 h, 48 h, 4 weeks, and 17 weeks posttransplantation. Immunocytochemistry for either a human nuclear antigen (SC101) or a human cytoplasmic antigen (SC121) revealed extensive human cell survival and engraftment within the injured mouse spinal cord. At 24 and 48 h posttransplantation, numerous human cells had migrated out from the injection site. By 17 weeks, many human cells had migrated away from the lesion epicenter, such that a clear injection site was no longer visible. SC121-immunopositive cells were found in both gray and white matter, and human cells were morphologically distinct depending on whether they were found within white matter or gray matter (Fig. 1). All hCNS-SCns- or hfibroblast-transplanted mice exhibited successful engraftment upon euthanasia. In sagittal sections, progeny of hCNS-SCns were found >1 cm from the lesion epicenter. Migration was greater rostral to the injection site, and migration into the site of injury was rare; a rim of spared tissue in the contused cord, even at the epicenter, was frequently observed (Fig. 6, which is published as supporting information on the PNAS web site). Myelination or sprouting/regeneration of spared axons in this region to form bridge circuits has been hypothesized to promote recovery of function after spinal cord injury.

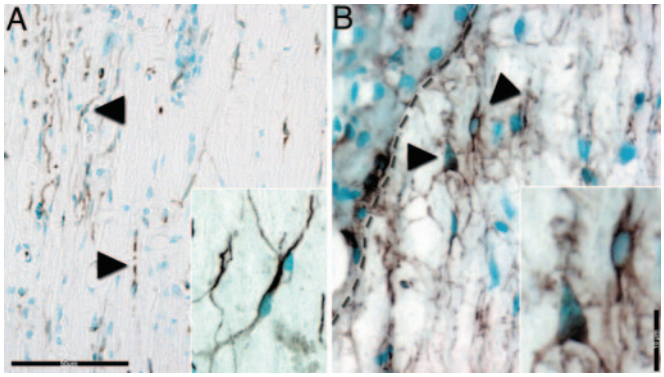

Fig. 1. The progeny of hCNS-SCns migrate and are morphologically distinct in gray vs. white matter. Shown are human immunopositive cells (SC121, brown) 17 weeks postgrafting. (*A*) In white matter, many human cells have an elongated, oligodendrocyte-like morphology (arrowheads). (*B*) In gray matter, some human cells exhibit neuronal morphologies (arrowheads); lesion perimeter is above and left of the dashed line. *Insets* in *A* and *B* show higher magnification of the morphologies adopted by human cells within white and gray matter, respectively. (Scale bars: 50 μm; *Insets*, 10 μm.)

hCNS-SCns Promote Locomotor Recovery. At 16 weeks postengraftment, BBB scoring suggested a recovery of coordinated forelimb–hindlimb locomotor function in 50-kd spinal cord-injured (SCI) hCNS-SCns-transplanted mice ($n = 11$) in comparison with vehicle controls ($n = 15$) (Fig. 2 *A* and *C*). χ^2 analysis of coordination recovery revealed a higher observed frequency of coordination (BBB score > 12) in hCNS-SCns vs. vehicle controls ($P < 0.05$; $\chi^2 = 3.94$). Repeated-measures ANOVA yielded a significant main effect for hCNS-SCns vs. vehicle control BBB performance, F (1, 24) = 2.28, $P < 0.01$, with a Cohen's effect size $d = -0.73$, indicating the effect was "moderately large" (Fig. 2*A*). Individual t tests showed significant differences between hCNS-SCns and vehicle control groups beginning at 6 weeks posttransplantation (asterisks in Fig. 2*A*; see also bold values in Table 1, which is published as supporting information on the PNAS web site). Additionally, a subset of mice tested on a linear quantitative horizontal ladder beam task also showed that hCNS-SCns-grafted mice ($n = 9$) exhibited significantly fewer errors than vehicle controls ($n = 12$), averaging 4.2 (SE ± 1.2) vs. 13.5 (SE ± 4.1) errors, respectively (Fig. 2*C*; Student's t test, $P < 0.05$).

To address the potential for any transplanted cell population to produce locomotor recovery in this paradigm and the reproducibility of these observations in a more severe injury model, we added a hfibroblast control and increased the injury severity to 60 kd (Fig. 2 *B* and *D*) in cohort 2. At 16 weeks postengraftment, BBB scoring suggested a recovery of stepping ability in 60-kd SCI hCNS-SCns-transplanted mice ($n = 8$) in comparison with vehicle ($n = 10$) or hfibroblast ($n = 8$) controls. χ^2 analysis revealed a higher observed frequency of stepping (BBB score > 11) in hCNS-SCns vs. vehicle ($P < 0.02$; $\chi^2 = 5.45$) or hfibroblast ($P < 0.05$; $\chi^2 = 4.00$) controls. hfibroblast and vehicle control groups were not significantly different from each other ($P < 0.80$; $\chi^2 = 0.06$). Repeated-measures ANOVA did not yield a significant main effect for the groups; however, individual t tests showed significant differences between hCNS-SCns and either vehicle or hfibroblast-transplanted controls beginning at 4 weeks postgrafting (asterisks in Fig. 2*B* and bold values in Table 1). Further, hCNS-SCns-grafted mice ($n = 8$) exhibited significantly fewer errors on the quantitative and more sensitive horizontal ladder beam task than vehicle controls ($n = 10$), averaging 9.9 (SE ± 1.2) vs. 17.4 (SE ± 3.6) errors (Fig. 2*D*; Student's t test, $P < 0.05$). hfibroblast controls ($n = 8$) did not differ

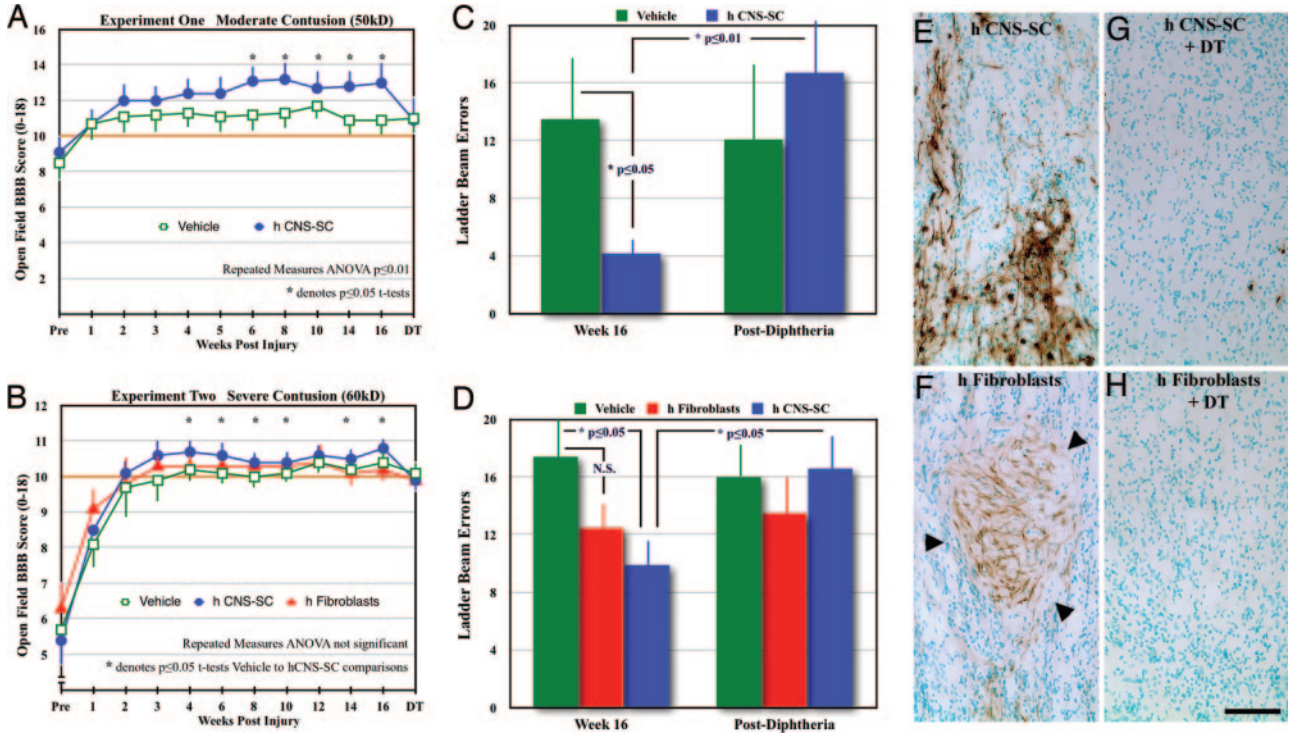

Fig. 2. Surviving hCNS-SCns promote locomotor recovery. (*A* and *B*) BBB locomotor performance is significantly improved in 50-kd SCI hCNS-SCns-grafted mice compared with vehicle controls (repeated-measures ANOVA, $P \leq 0.01$) (*A*) and in 60-kd SCI hCNS-SCns-grafted mice compared with vehicle or hfibroblast controls (*B*) in individual t tests of recovery times. Asterisks indicate *t* test ($P \leq 0.05$). DT was administered after 16-week BBB scores were obtained. (*C* and *D*) Errors on a ladder beam task are significantly decreased in 50-kd SCI hCNS-SCns-grafted mice compared with vehicle controls ($P \leq 0.05$) (*C*) and in 60-kd SCI hCNS-SCns-grafted mice compared with vehicle controls ($P \leq 0.05$) (*D*). No significant differences were observed between either vehicle vs. hfibroblasts ($P \leq 0.87$) or hfibroblasts vs. hCNS-SCns, although there was a trend toward the latter ($P \leq 0.17$). Open-field BBB and ladder beam improvements in hCNS-SCns-transplanted mice were reversed 1 week after treatment with DT in *A–D*. (*E–H*) hCNS-SCns (*E*) or human hfibroblasts (*F*) 17 weeks posttransplantation after treatment with vehicle in comparison with DT (*G* and *H*), which ablated the majority of human cells. No evidence of toxicity to surrounding host tissues was apparent. See Fig. 7 for additional photos.

from vehicle controls, averaging 12.5 (SE ± 2.1) errors (Student's *t* test, $P < 0.87$), but approached significance in comparison with hCNS-SCns-grafted mice (Student's *t* test, $P < 0.17$). To our knowledge, this is the longest time that mice receiving stem cell grafts of any type have been tracked behaviorally.

To investigate the effect of selective ablation of engrafted hCNS-SCns on locomotor recovery, we treated animals with DT after behavioral recovery stabilized and reassessed locomotor performance on the BBB and ladder beam 1 week later. Murine cells are 100,000 times less sensitive to DT than are human cells (19), and DT has been used extensively as a tool for targeted cell ablation in transgenic rodent models. These models either conditionally drive DT A-chain expression in specific subpopulations of cells or express the human DT receptor under a promoter that is specific to a selective cell population. DT-targeted cells die by means of apoptosis with little or no effects on nontargeted cells and neighboring tissues (20–22). Grafted mice that received vehicle retained an extensive number of hCNS-SCns (Fig. 2*E*) or hfibroblasts (Fig. 2*F*), whereas grafted mice that received DT had few or no remaining human cells (Fig. 2 *G* and *H*; see also Fig. 7, which is published as supporting information on the PNAS web site). Vehicle-treated hCNS-SCns-transplanted mice were unaffected or improved slightly, whereas DT-treated hCNS-SCns-transplanted mice showed significant decrements on both the BBB and ladder beam (Fig. 2 *A–D* and Table 1). Comparable results were observed in both the 50-kd (Fig. 2 *A* and *C*) and 60-kd SCI cohorts (Fig. 2 *B* and *D*). No significant differences in behavioral performance were observed after DT treatment in mice transplanted with hfibroblasts as a cellular control in the 60-kd SCI groups (Fig. 2 *B* and *D*), suggesting that a general toxic effect of cell ablation on host locomotor function is unlikely.

hCNS-SCns Do Not Contribute to the Glial Scar. Tissue from mice 4 and 17 weeks posttransplantation was examined for differentiation markers for astrocyte, neuron, and oligodendrocyte lineages. Surprisingly, few GFAP-immunopositive astrocytes colocalized with either human specific nuclear (SC101) or cytoplasmic (SC121) markers (Fig. 3*A*), and only 2.9% (SD = 4.1) of SC121-immunopositive cells exhibited double labeling for GFAP in confocal images 17 weeks posttransplantation. Many animals, in fact, contained no detectable human cells colocalized with GFAP. Further, using an antibody specific to human-GFAP (SC123), we rarely detected human cells that had differentiated into SC123-positive astrocytes (Fig. 8*D*, which is published as supporting information on the PNAS web site). We did not observe that hCNS-SCns formed a border surrounding the lesion area or appeared to contribute to a glial scar. These data suggest that few engrafted human cells differentiated into GFAP-positive astrocytes into the immunodeficient NOD-*scid* mouse.

hCNS-SCns Differentiate into Neurons and Form Synapses. On average, 26.4% (SD = 22.0) of SC121-immunopositive human cells exhibited double labeling for β-tubulin III. Infrequent glutamate decarboxylase (GAD)-67-immunopositive neurons were colocalized with human nuclei (SC101) (Fig. 3*B*). We also detected NeuN-positive nuclei colocalized with human cytoplasm (Fig. 3*C*). GAD-67- and NeuN-positive cells were observed only in gray matter. These data suggest that hCNS-SCns are capable of terminal

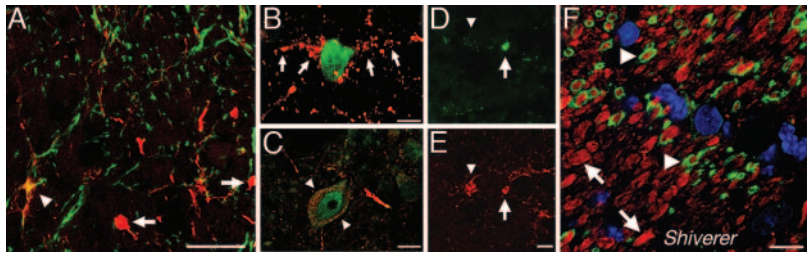

Fig. 3. Differentiation of hCNS-SCns into astrocytes, neurons, and oligodendrocytes at 17 weeks. (*A*) Few human cytoplasm-positive (SC121, red), GFAP-positive (green) astrocytes (arrowheads) could be detected. Most human cells were negative for GFAP (arrows). (*B*) Glutamate decarboxylase (GAD)-67-immunopositive (red) processes (arrows) were occasionally colocalized with human nuclei (SC101, green), indicating GABAergic neurons. (*C*) Human cytoplasm-positive cell (red) colocalized (arrowheads) with the neural marker NeuN (green). (*D* and *E*) Several APC-positive oligodendrocytes (red), one (arrow) colocalized with a human nuclei (SC101, green). Other APC-positive cells (arrowhead) were not colocalized. (*F*) Injection of hCNS-SCns into neonatal NOD-*scid*/*shi* mice demonstrated MBP (green, arrowheads) wrapping neurofilament-positive mouse axons (red) in the cerebellum. Other axons remained dysmyelinated (arrows). Blue nuclei are Hoechst-stained. (Scale bars: *A*, *D*, and *E*, 20 μm; *B*, *C*, and *F*, 10 μm.)

differentiation along a neural lineage (see also Fig. 9, which is published as supporting information on the PNAS web site). To verify terminal differentiation of hCNS-SCns to neurons, we used immuno-EM in tissue labeled for SC121. SC121-positive neuronal structures were detected at the EM level, and evidence of newly differentiated human neurons sending processes into the mouse parenchyma (Fig. 4 *A* and *B*) and forming putative synapses with the mouse host (Fig. 4 *C* and *D*) was observed. Fig. 4 *C* and *D* shows all of the ultrastructural criteria for synapses between grafted cells and host, including membrane thickening and apposition, pre- and postsynaptic densities, a synaptic cleft, and synaptic vesicles. The close association of human cells exhibiting neuronal morphologies with mouse axons is supported by immunocytochemical evidence that hCNS-SCns are capable of terminal neuronal differentiation.

hCNS-SCns Differentiate into Oligodendrocytes and Myelinate. At 4 weeks posttransplantation, we detected numerous hCNS-SCns colocalized with anti-NG2, an early marker for oligodendroglial progenitors. NG2-positive, human antigen-positive cells were found predominantly in white matter. At 17 weeks, both NG2- and CC-1/APC-positive cells were colocalized with human nuclei (Fig. 3 *D* and *E*), suggesting differentiation of engrafted cells along an oligodendroglial lineage. Of the SC121-immunopositive human cells, 64.1% (SD = 23.1) were double-labeled for CC-1/APC, suggesting robust terminal differentiation to oligodendrocytes. Using Hoechst counterstaining, we never observed human immunopositive cells with two nuclei, suggesting that cell fusion, if it occurred at all, was a very rare event.

Because of the number of hCNS-SCns observed to express oligodendroglial lineage markers, we used three approaches to test the hypothesis that hCNS-SCns could myelinate axons *in vivo*. We first crossed NOD-*scid* with *shiverer* (*shi*) mice, which have a partial deletion in the gene for MBP. hCNS-SCns were transplanted into

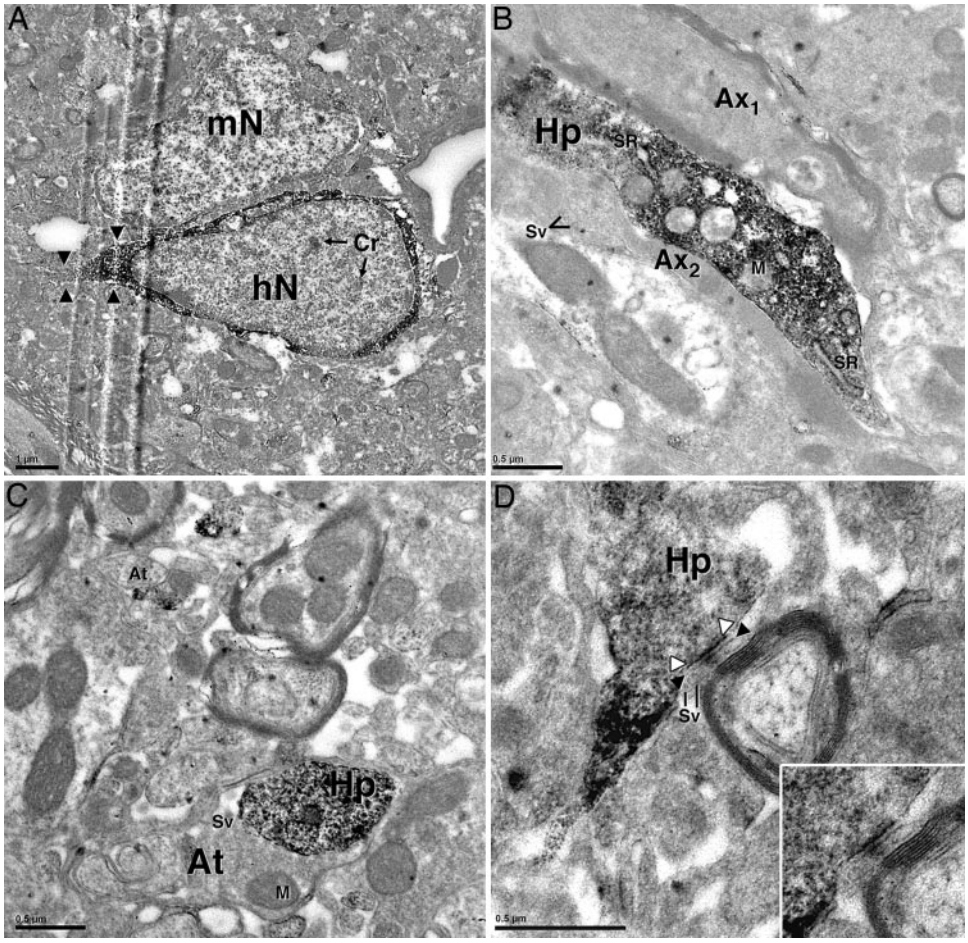

Fig. 4. EM of differentiation of hCNS-SCns into putative neurons. Immuno-EM for the human cytoplasm marker SC121 reveals many engrafted cells within the spinal neuropil. (*A*) Nucleus of a human cytoplasm-labeled cell adjacent to the nucleus of an endogenous mouse cell (mN). Human positive perikaryal cytoplasm surrounds the nucleus (hN), which exhibits patchy chromatin aggregates (Cr) typical of neurons. A single apical process (arrowheads), together with the paucity of cytoplasm, suggests that this human cell could be an immature neuron. (*B*) Transverse section of two axons and a human cytoplasm-labeled process (Hp). The upper axon (Ax_1) is myelinated; the lower axon (Ax_2) is not. Ax_2 exhibits a bouton-like swelling containing synaptic vesicles (Sv) in apposition with structure Hp; the presence of mitochondria (Mt) and smooth endoplasmic reticulum (SR) within Hp suggests that this process may be a dendrite. (*C*) Human cytoplasm-labeled process (Hp) cradled by a mouse axon terminal (At). Synaptic vesicles (Sv) and a single mitochondrion (M) are visible in the mouse axon terminal in close apposition with structure Hp; there are no interposing membranes between Hp and At, but no cleft is visible. (*D*) Human cytoplasm-labeled process (Hp) forming a putative symmetric synapse with a mouse axon terminal. There is thickening of both the presynaptic (black arrowheads) and postsynaptic (white arrowheads) membranes, with widening of membrane apposition and greater electron density within the cleft. Synaptic vesicles (Sv) are present within the mouse axon terminal. *Inset* shows the ''synapse region'' without overlays.

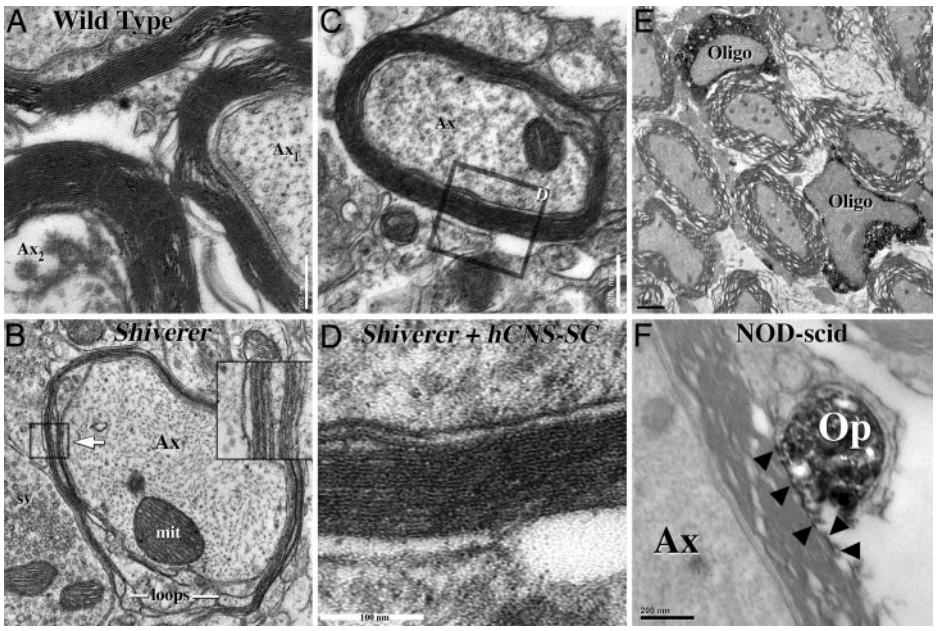

Fig. 5. EM of myelination by hCNS-SCns in the spinal cord. Six-week-old NOD-*scid*/*shi* mice were grafted with hCNS-SCns after a contusion injury and examined at 10 weeks of age. (*A*) Normal myelination of axons (Ax) within the dorsal funiculus of heterozygous *shiverer* littermates. (*B*) Spinal cord from ungrafted NOD-*scid*/*shi* reveals hypomyelination (*Inset* shows eight lamellae), loops of myelin, and a lack of the major dense line but healthy mitochondria (mit). (*C*) Spinal cord from a hCNS-SCns-grafted NOD-*scid*/*shi* mouse demonstrating thicker, dense myelination. (*D*) Boxed area in *C* showing compact myelin, >20 lamellae, and presence of the major dense line. (*E*) In spinal cord of contusion-injured NOD-*scid* mice, immuno-EM for human cytoplasm (SC121) reveals grafted human stem cells 17 weeks after spinal cord injury. Two human oligodendrocytes (Oligo) appear associated with neighboring axons. (*F*) Cross section of a human immunopositive oligodendrocytic tongue process (Op) and residual immunopositive cytoplasm within the outermost wrap of myelin (arrowheads). (Scale bars: *A–C* and *F*, 200 nm; *D*, 100 nm; *E*, 1 μm.)

the cerebella of NOD-*scid*/*shi* mice at postnatal day 1. At this early stage of development, myelination is just beginning; therefore, hCNS-SCns would encounter the fewest obstacles to integrating with host axons. In ungrafted NOD-*scid*/*shi* mice, an antibody against the deleted portion of MBP did not detect mouse myelin, as expected. In contrast, in the cerebella of NOD-*scid*/*shi* mice transplanted with hCNS-SCns, MBP staining was detected surrounding many neurofilament-positive axons, suggesting that engrafted human cells differentiated into mature oligodendrocytes capable of expressing normal MBP and integrating with mouse axons (Fig. 3*F*).

We next transplanted hCNS-SCns into contusion-injured spinal cords of young adult NOD-*scid*/*shi* mice and used EM to investigate myelination in the dorsal funiculus of the spinal cord. Wild-type and heterozygous uninjured NOD-*scid*/*shi* mice have normal myelination and frequently exhibit >25 wraps of myelin per axon (Fig. 5*A*). Ungrafted, contusion-injured NOD-*scid*/*shi* mice never exhibited more than nine lamellae per axon (Fig. 5*B*), consistent with previous characterizations of homozygous *shi* mice (23, 24). In contrast, 6-week-old, contusion-injured NOD-*scid*/*shi* mice transplanted with hCNS-SCns ($n = 5$) exhibited axons ensheathed in >20 lamellae of myelin by 4 weeks posttransplantation (Fig. 5 *C* and *D*), suggesting terminal oligodendrocyte differentiation by human cells.

Finally, to demonstrate more conclusively that human cells are capable of remyelination in animals with normal MBP/myelination before injury, we examined contusion-injured NOD-*scid* mice by using preembedding immuno-EM. Ungrafted NOD-*scid* mice did not exhibit staining for human cells at the light or EM level. In contrast, all NOD-*scid* SCI mice transplanted with hCNS-SCns and examined at the EM level exhibited human cytoplasm-positive staining (SC121) within oligodendrocytes closely associated with axons (Fig. 5*E*). Additionally, we found human-labeled oligodendrocytic tongue processes extending to ensheath unlabeled mouse axons (Fig. 5*F*), strongly suggesting active remyelination of mouse axons by engrafted hCNS-SCns.

Discussion

Role of hCNS-SCns in Spinal Cord Injury Repair. Hypothetically, cell-based therapeutics for spinal cord injury could affect histological and/or functional outcome in a number of ways: (*i*) differentiation and functional integration of new cells into spared spinal cord circuitry (e.g., forming new oligodendrocytes and/or neurons), (*ii*) increasing host neuronal, oligodendroglial, or axonal survival or decreasing host glial scaring, and (*iii*) increasing host-mediated regeneration or remyelination. The possibility that hCNS-SCns affect host locomotor recovery by means of multiple mechanisms must also be considered.

The observed reversal of locomotor improvement in DT-treated, hCNS-SCns-engrafted, SCI NOD-*scid* mice suggests that hCNS-SCns survival in the host plays a role in the maintenance of improved performance. One caveat is the potential for cell ablation to have caused extraneous damage to host cells/tissue, affecting behavioral performance nonspecifically. The extensive characterization of DT cell ablation as apoptotic and nondamaging to surrounding tissues in previous studies (20–22), lack of observed damage to the host neuropil, and lack of a DT treatment effect on behavioral performance in hfibroblast-grafted animals suggests that nonspecific toxicity is unlikely. Additionally, the probable source of such a nonspecific effect is activation of the host immune response, which would be mitigated in NOD-*scid* mice. Acute withdrawal of hCNS-SCns-derived trophic support could also affect host cell function and lead to decrements in behavioral performance, but this possibility is mitigated by the long-term behavioral plateau before DT treatment in this study. Further studies to identify additional or alternative mechanisms of recovery are needed, and the post-DT period should be lengthened by using younger NOD-*scid* animals. However, taken together, these data suggest that hCNS-SCns differentiation to myelinating oligodendrocytes and neurons with EM criteria for host synaptic connections could be mechanisms for sustained locomotor recovery in this model.

hCNS-SCns-Mediated Remyelination. We report that transplanted hCNS-SCns can remyelinate axons, both in naïve NOD-*scid*/*shi* CNS and in injured NOD-*scid*/*shi* and NOD-*scid* spinal cord. To our knowledge, these data are the first to demonstrate remyelination by engrafted human neural stem cells in a traumatic spinal cord injury model, although previous studies have shown the capacity for stem cells to myelinate in atraumatic models of CNS demyelination and disease. Transplanted adult rat neurospheres in an experimental autoimmune encephalomyelitis model are associated with remyelination and functional recovery (25). Similarly, rat CNS precursors identified as Schwann cells and some oligodendrocytes

remyelinated rat spinal cord axons in focal chemical demyelination models (26). Additionally, predifferentiation of cultured mouse or human ES cells to generate "oligospheres" before transplantation has been reported to yield engrafted cells expressing mature oligodendrocyte differentiation markers in association with *in vivo* remyelination (12, 27, 28). Finally, direct or i.v. injection of bone marrow-derived stem cells has been reported to result in remyelination in focal demyelination models (29, 30); however, the origin of the remyelinating cells is unclear, and the stimulation of a host remyelination response has not been ruled out.

hCNS-SCns-Mediated Human–Mouse Synapse Formation. We present data supporting the potential for human stem cells to form synapses with the host in the injured spinal cord. Previous studies have shown that both naïve and neuronal differentiated rodent ES cells can form synapses with rat or mouse host neurons, respectively, and that these cells are functional based on electrophysiological recording (31, 32). Additionally, mouse and rat CNS neural precursors can form synapses with same-species host cells after transplantation, based on electrophysiology (33) or EM analysis (34). Similarly, it has been reported recently that human neural stem cells form synapses at the EM level after transplantation into a gerbil brain ischemia model (35). At present, whether sufficient human–mouse synaptic connections are established by hCNS-SCns in our paradigm to account for the locomotor recovery observed is not clear, and electrophysiological evidence for functional circuit integration will be required to ascertain the net impact of these connections for the host.

Immunosuppression Models and Xenografts. Immunosuppression for graft survival is an issue that affects all neurotransplantation research, particularly xenograft studies. Although immunosuppressants are routinely used to prevent clinical allograft rejection, these drugs may fail to provide long-term protection from xenograft rejection (36). To minimize xenotransplantation barriers for long-term engraftment after spinal cord injury, we chose the NOD-*scid* mouse (37). Stem cells, including neurospheres, can respond to chemokine signaling (38, 39); consequently, both constitutive immunodeficiency and pharmacological immunosuppression could affect the engraftment, migration, and differentiation of transplanted cells. Additionally, the lack of a fully functional immune system in NOD-*scid* mice could affect the evolution of spinal cord injury; however, the gross histology of the lesion in Nod-*scid* mice does not differ dramatically from other mouse strains, and NOD-*scid* mice exhibit clear and sustained locomotor impairments after spinal cord injury. Further, the NOD-*scid* mouse model avoids the confound of cellular toxicity associated with pharmacological immunosuppression.

Conclusions

These results suggest that hCNS-SCns are capable of surviving and differentiating in a traumatically injured environment without contributing to glial scarring. Selective ablation of these cells suggests that hCNS-SCns play a role in locomotor recovery. Recently, these hCNS-SCns have also been shown to engraft in a model of ischemia/reperfusion/stroke (38). Together, these findings suggest that hCNS-SCns could have potential benefits for multiple CNS diseases and injuries. However, this study represents an initial step toward defining potential clinical applications; additional animal studies are necessary both to establish the mechanism(s) of recovery and to evaluate the potential of these cells for possible therapeutic use.

We thank Edwin Apilado, Monika Dohse, Dongping He, Ilse Kraxberger, Hong-Li Lui, Rebecca Nishi, Richard Silva, Yumin Tang, Tanya Thamkruphat, and Robert Tushinski for technical assistance. This work was supported by National Institutes of Health Grants R43NS046975 and R01NS049885 and the Christopher Reeve Foundation.

1. Taupin, P. & Gage, F. H. (2002) *J. Neurosci. Res.* **69,** 745–749.
2. Cao, Q., Benton, R. L. & Whittemore, S. R. (2002) *J. Neurosci. Res.* **68,** 501–510.
3. Cao, Q. L., Zhang, Y. P., Howard, R. M., Walters, W. M., Tsoulfas, P. & Whittemore, S. R. (2001) *Exp. Neurol.* **167,** 48–58.
4. Wu, S., Suzuki, Y., Kitada, M., Kitaura, M., Kataoka, K., Takahashi, J., Ide, C. & Nishimura, Y. (2001) *Neurosci. Lett.* **312,** 173–176.
5. Vroemen, M., Aigner, L., Winkler, J. & Weidner, N. (2003) *Eur. J. Neurosci.* **18,** 743–751.
6. Cao, Q. L., Howard, R. M., Dennison, J. B. & Whittemore, S. R. (2002) *Exp. Neurol.* **177,** 349–359.
7. Wictorin, K. & Bjorklund, A. (1992) *NeuroReport* **3,** 1045–1048.
8. Stepanov, G. A., Karpenko, D. O., Aleksandrova, M. A., Podgornyi, O. V., Poltavtseva, R. A., Pevishchin, A. V., Marey, M. V. & Sukhikh, G. T. (2003) *Bull. Exp. Biol. Med.* **135,** 397–400.
9. Akesson, E., Holmberg, L., Jonhagen, M. E., Kjaeldgaard, A., Falci, S., Sundstrom, E. & Seiger, A. (2001) *Exp. Neurol.* **170,** 305–316.
10. Saporta, S., Kim, J. J., Willing, A. E., Fu, E. S., Davis, C. D. & Sanberg, P. R. (2003) *J. Hematother. Stem Cell Res.* **12,** 271–278.
11. Saporta, S., Makoui, A. S., Willing, A. E., Daadi, M., Cahill, D. W. & Sanberg, P. R. (2002) *J. Neurosurg.* **97,** 63–68.
12. Keirstead, H. S., Nistor, G., Bernal, G., Totoiu, M., Cloutier, F., Sharp, K. & Steward, O. (2005) *J. Neurosci.* **25,** 4694–4705.
13. Iwanami, A., Kaneko, S., Nakamura, M., Kanemura, Y., Mori, H., Kobayashi, S., Yamasaki, M., Momoshima, S., Ishii, H., Ando, K., *et al.* (2005) *J. Neurosci. Res.* **80,** 182–190.
14. Tamaki, S., Eckert, K., He, D., Sutton, R., Doshe, M., Jain, G., Tushinski, R., Reitsma, M., Harris, B., Tsukamoto, A., *et al.* (2002) *J. Neurosci. Res.* **69,** 976–986.
15. Uchida, N., Buck, D. W., He, D., Reitsma, M. J., Masek, M., Phan, T. V., Tsukamoto, A. S., Gage, F. H. & Weissman, I. L. (2000) *Proc. Natl. Acad. Sci. USA* **97,** 14720–14725.
16. Basso, D. M., Beattie, M. S. & Bresnahan, J. C. (1995) *J. Neurotrauma* **12,** 1–21.
17. Dergham, P., Ellezam, B., Essagian, C., Avedissian, H., Lubell, W. D. & McKerracher, L. (2002) *J. Neurosci.* **22,** 6570–6577.
18. Anderson, A. J., Cummings, B. J. & Cotman, C. W. (1994) *Exp. Neurol.* **125,** 286–295.
19. Pappenheimer, A. M., Jr., Harper, A. A., Moynihan, M. & Brockes, J. P. (1982) *J. Infect. Dis.* **145,** 94–102.
20. Saito, M., Iwawaki, T., Taya, C., Yonekawa, H., Noda, M., Inui, Y., Mekada, E., Kimata, Y., Tsuru, A. & Kohno, K. (2001) *Nat. Biotechnol.* **19,** 746–750.
21. Drago, J., Padungchaichot, P., Wong, J. Y., Lawrence, A. J., McManus, J. F., Sumarsono, S. H., Natoli, A. L., Lakso, M., Wreford, N., Westphal, H., *et al.* (1998) *J. Neurosci.* **18,** 9845–9857.
22. Cailhier, J. F., Partolina, M., Vuthoori, S., Wu, S., Ko, K., Watson, S., Savill, J., Hughes, J. & Lang, R. A. (2005) *J. Immunol.* **174,** 2336–2342.
23. Privat, A., Jacque, C., Bourre, J. M., Dupouey, P. & Baumann, N. (1979) *Neurosci. Lett.* **12,** 107–112.
24. Inoue, Y., Inoue, K., Terashima, T., Mikoshiba, K. & Tsukada, Y. (1983) *Anat. Embryol.* **168,** 159–171.
25. Pluchino, S., Quattrini, A., Brambilla, E., Gritti, A., Salani, G., Dina, G., Galli, R., Del Carro, U., Amadio, S., Bergami, A., *et al.* (2003) *Nature* **422,** 688–694.
26. Keirstead, H. S., Ben-Hur, T., Rogister, B., O'Leary, M. T., Dubois-Dalcq, M. & Blakemore, W. F. (1999) *J. Neurosci.* **19,** 7529–7536.
27. Liu, S., Qu, Y., Stewart, T. J., Howard, M. J., Chakrabortty, S., Holekamp, T. F. & McDonald, J. W. (2000) *Proc. Natl. Acad. Sci. USA* **97,** 6126–6131.
28. Nistor, G. I., Totoiu, M. O., Haque, N., Carpenter, M. K. & Keirstead, H. S. (2004) *Glia* **49,** 385–396.
29. Akiyama, Y., Radtke, C. & Kocsis, J. D. (2002) *J. Neurosci.* **22,** 6623–6630.
30. Sasaki, M., Honmou, O., Akiyama, Y., Uede, T., Hashi, K. & Kocsis, J. D. (2001) *Glia* **35,** 26–34.
31. Harkany, T., Andang, M., Kingma, H. J., Gorcs, T. J., Holmgren, C. D., Zilberter, Y. & Ernfors, P. (2004) *J. Neurochem.* **88,** 1229–1239.
32. Wernig, M., Benninger, F., Schmandt, T., Rade, M., Tucker, K. L., Bussow, H., Beck, H. & Brustle, O. (2004) *J. Neurosci.* **24,** 5258–5268.
33. Auerbach, J. M., Eiden, M. V. & McKay, R. D. (2000) *Eur. J. Neurosci.* **12,** 1696–1704.
34. Snyder, E. Y., Yoon, C., Flax, J. D. & Macklis, J. D. (1997) *Proc. Natl. Acad. Sci. USA* **94,** 11663–11668.
35. Ishibashi, S., Sakaguchi, M., Kuroiwa, T., Yamasaki, M., Kanemura, Y., Shizuko, I., Shimazaki, T., Onodera, M., Okano, H. & Mizusawa, H. (2004) *J. Neurosci. Res.* **78,** 215–223.
36. Larsson, L. C., Frielingsdorf, H., Mirza, B., Hansson, S. J., Anderson, P., Czech, K. A., Strandberg, M. & Widner, H. (2001) *Exp. Neurol.* **172,** 100–114.
37. Greiner, D. L., Hesselton, R. A. & Shultz, L. D. (1998) *Stem Cells* **16,** 166–177.
38. Kelly, S., Bliss, T. M., Shah, A. K., Sun, G. H., Ma, M., Foo, W. C., Masel, J., Yenari, M. A., Weissman, I. L., Uchida, N., *et al.* (2004) *Proc. Natl. Acad. Sci. USA* **101,** 11839–11844.
39. Ji, J. F., He, B. P., Dheen, S. T. & Tay, S. S. (2004) *Neurosci. Lett.* **355,** 236–240.